2018

RNA ligase-like domain in activating signal cointegrator 1 complex subunit 1 (ASCC1) regulates ASCC complex function during alkylation damage

Jennifer M. Soll

Joshua R. Brickner

Miranda C. Mudge

Nima Mosammaparast

RNA ligase-like domain in activating signal cointegrator 1 complex subunit 1 (ASCC1) regulates ASCC complex function during alkylation damage

Jennifer M. Soll[1], **Joshua R. Brickner**[2], **Miranda C. Mudge**, and **Nima Mosammaparast**[3]

From the Department of Pathology and Immunology, Division of Laboratory and Genomic Medicine, Washington University in St. Louis, St. Louis, Missouri 63110

Edited by Patrick Sung

Multiple DNA damage response (DDR) pathways have evolved to sense the presence of damage and recruit the proper repair factors. We recently reported a signaling pathway induced upon alkylation damage to recruit the AlkB homolog 3, α-ketoglutarate–dependent dioxygenase (ALKBH3)–activating signal cointegrator 1 complex subunit 3 (ASCC3) dealkylase–helicase repair complex. As in other DDR pathways, the recruitment of these repair factors is mediated through a ubiquitin-dependent mechanism. However, the machinery that coordinates the proper assembly of this repair complex and controls its recruitment is still poorly defined. Here, we demonstrate that the ASCC1 accessory subunit is important for the regulation of ASCC complex function. ASCC1 interacts with the ASCC complex through the ASCC3 helicase subunit. We find that ASCC1 is present at nuclear speckle foci prior to damage, but leaves the foci in response to alkylation. Strikingly, ASCC1 loss significantly increases ASCC3 foci formation during alkylation damage, yet most of these foci lack ASCC2. These results suggest that ASCC1 coordinates the proper recruitment of the ASCC complex during alkylation, a function that appears to depend on a putative RNA-binding motif near the ASCC1 C terminus. Consistent with its role in alkylation damage signaling and repair, ASCC1 knockout through a CRISPR/Cas9 approach results in alkylation damage sensitivity in a manner epistatic with ASCC3. Together, our results identify a critical regulator of the ALKBH3–ASCC alkylation damage signaling pathway and suggest a potential role for RNA-interacting domains in the alkylation damage response.

Endogenous DNA alkylation damage is caused by numerous agents that are present in the environment, as well as by cellular metabolism (1–3). Exogenous alkylation damage may be induced by a number of cancer chemotherapeutics. If left unrepaired, alkylated adducts can stall replication, cause mutations, and potentially lead to cell death. Because of the diverse chemical nature of alkylation damage, multiple pathways have evolved to protect the genome from alkylation damage. These include base-excision repair (BER),[4] direct reversal by O^6-methylguanine methyltransferase (MGMT), and the AlkB family of demethylases/dealkylases (1, 2, 4).

Although BER excises alkylated bases, it is also responsible for the removal of many other forms of DNA damage, including oxidized bases, uracil, and other deaminated bases (5). Conversely, MGMT and the AlkB proteins appear to be dedicated solely to the direct reversal of alkylation damage (1, 2, 4). MGMT repairs O-linked adducts by the direct transfer of an alkyl group to a cysteine in the active site via a nonenzymatic mechanism that inactivates MGMT (6, 7). AlkB proteins, however, are *bona fide* demethylases/dealkylases that directly reverse N-linked adducts such as 1-methyladenine (1meA) and 3-methylcytosine (3meC) in an Fe(II) and 2-oxoglutarate–dependent reaction (8, 9). 1meA and 3meC are particularly cytotoxic as both disrupt canonical base pairing, hence blocking replicative DNA polymerases (2). In humans, there are nine AlkB homologs (10–12), but only two of these proteins, ALKBH2 and ALKBH3, have been shown to repair 1meA and 3meC in DNA (13).

It is important for the cell to coordinate the various alkylation repair pathways, as there is some redundancy in the substrate binding of the numerous repair factors. This overlap in substrate preference may lead to a potential conflict during initial lesion recognition and reduce the efficiency of repair. For example, alkyl-adenine glycosylase (AAG and N-methylpurine DNA glycosylase), which is involved in initiating BER, binds to the 3,N^4-ethenocytosine (ϵC) lesion but cannot excise the base (14, 15). Interestingly, ALKBH2 is capable of repairing ϵC but is inhibited by the presence of AAG (16). Because of such compe-

tition, it is important for the cell to have a tightly controlled damage response to ensure that repair occurs in an efficient manner, while simultaneously preventing recruitment of inappropriate repair factors. To understand the interplay between these different repair mechanisms, it is first necessary to determine the regulation of the individual alkylation damage repair pathways. However, for alkylation damage repair, little is known about the regulation of repair factor recruitment *in vivo*.

We and others previously found that the ALKBH3 demethylase associates with the Activation Signal Cointegrator Complex (ASCC, also known as ASC-1) (17, 18), which plays a key role in repairing alkylated DNA in cell lines overexpressing ALKBH3, such as prostate and non-small cell lung tumor cells (18–20). ASCC is composed of three proteins: ASCC1, ASCC2, and ASCC3 (also known as p50, p100, and p200, respectively) (17). Biochemical characterization of this complex revealed that ASCC3 is a DNA helicase, whose unwinding activity is crucial for dealkylation by the ALKBH3 repair enzyme *in vitro* (18). It is thought that ASCC3 and ALKBH3 work in concert such that ASCC3 generates the single-stranded substrate needed for ALKBH3-mediated repair. Recently, we found that ASCC2 is important for the recruitment of the ALKBH3–ASCC3 complex to nuclear speckle foci specifically during alkylation damage (21). This recruitment depends upon nonproteasomal Lys-63–linked ubiquitination by the E3 ligase RNF113A (21). The ubiquitination is recognized by the ASCC2 subunit, which is responsible for the recruitment of both ASCC3 and ALKBH3 to sites of damage. Loss of ASCC2 results in increased sensitivity to alkylating agents, strongly suggesting that ASCC2-mediated recruitment is critical for efficient repair (21).

Here, we characterize ASCC1, the smallest subunit of the ASCC complex. We find that ASCC1, unlike ASCC2 or ASCC3, is constitutively present at nuclear speckle foci, yet it is removed from these nuclear regions upon alkylation damage. As a result, ASCC1 is capable of modulating ASCC3 recruitment during alkylation damage. This behavior of ASCC1 depends upon its C-terminal RNA ligase-like domain. Together, our data suggest a novel regulatory mechanism for the ALKBH3–ASCC repair pathway wherein ASCC1 modulates the localization and function of the complex components.

Results

ASCC1 interacts directly with ASCC3 but is present at nuclear speckle foci in the absence of damage

We wished to determine what factors associated with the ASCC complex are involved in regulating its function in response to alkylation damage. To this end, we focused on ASCC1, a protein previously shown to copurify with ASCC2 and ASCC3 (17, 18). To determine how the individual complex components associate with one another, we performed immunoprecipitation of HA-ASCC1 and HA-ASCC2 (Fig. 1A). Both of these factors coimmunoprecipitated ASCC3 from 293T cells. Consistent with this, immunoprecipitation of endogenous ASCC3 from 293T cell extracts yielded ASCC1, suggesting that this physical interaction is present at the endogenous level (Fig. 1B). To test whether ASCC1 and ASCC3 interact

directly, we purified all three components of the complex as recombinant proteins. His-tagged ASCC3 bound to immobilized GST-tagged ASCC1, as well as GST-ASCC2, but not GST alone (Fig. 1C). An N-terminal truncation of ASCC3 (NΔ-ASCC3; residues 401–2202) abrogated the interaction with ASCC2 but did not affect ASCC1 binding (Fig. 1C). Thus, both ASCC1 and ASCC2 can bind directly to ASCC3, but likely through distinct regions within ASCC3. Recombinant ASCC1 and ASCC2 did not interact with each other in pulldown assays (Fig. S1A), suggesting that ASCC3 serves as a scaffold between ASCC1 and ASCC2. To test this, we knocked out ASCC3 in PC-3 cells using CRISPR/Cas9 (Fig. S1B). Immunoprecipitation of HA-ASCC1 from parental PC-3 cells yielded the other two components of the complex, but ASCC2 was not coimmunoprecipitated in the absence of ASCC3 (Fig. 1D). Thus, ASCC3 is required to bridge the interaction between ASCC1 and ASCC2 *in vivo*.

As both ASCC2 and ASCC3 form nuclear foci specifically upon alkylation damage (21), and in light of the physical interactions between the complex components, we reasoned that ASCC1 may also form alkylation-induced foci (Fig. S1, *C and D*). However, HA-tagged ASCC1 formed foci that colocalized with the nuclear speckle component PRP8 in the absence of any damage (Fig. 1, *E and F*, and Fig. S1E). Surprisingly, treatment of the cells with the alkylating agent methyl methanesulfonate (MMS) significantly reduced ASCC1 colocalization with these nuclear domains in a time-dependent manner. This was not due to a reduction in the expression level of the tagged ASCC1 during MMS treatment (Fig. S1F). Taken together, these results suggest that ASCC1 is part of the ASCC complex but may perform a distinct function in response to alkylation damage.

ASCC1 modulates alkylation-induced ASCC3 foci formation

We next wished to determine the role of ASCC1 in ASCC3 foci formation. To this end, we knocked out ASCC1 in U2OS cells using CRISPR/Cas9 (Fig. S2, *A and B*). Interestingly, loss of ASCC1 significantly increased MMS-induced ASCC3 foci formation (Fig. 2, *A and B*). This increase was apparent with two different knockout clones, making it unlikely that the induction of foci was due to an off-target effect of CRISPR/Cas9. These results were not attributable to an increase of ASCC3 foci at baseline (*i.e.* without MMS) in the ASCC1 KO cells (Fig. S2C). In time-course experiments, ASCC3 foci were still resolved in the absence of ASCC1 upon removal of MMS (Fig. S2C). These results suggested that ASCC1 modulates ASCC3 foci formation during alkylation damage.

We next asked whether ASCC1 affects the colocalization of other components of the ASCC complex. Upon MMS treatment, nearly 75% of WT cells had colocalizing ASCC3 and HA-ASCC2 foci (Fig. 2, *C and D*). Under the same conditions, ASCC1 KOs had significantly fewer cells with colocalizing HA-ASCC2 and ASCC3 foci (42%). This was not due to a difference in the expression level of HA-ASCC2 in parental *versus* ASCC1 KO cells (Fig. S2D). This suggested that ASCC1 may function to promote colocalization of the other two components during alkylation damage. To test this biochemically, we immunoprecipitated endogenous ASCC2 in WT *versus* ASCC1 knockout PC-3 cells (Fig. S2E). Consistent with the diminished interac-
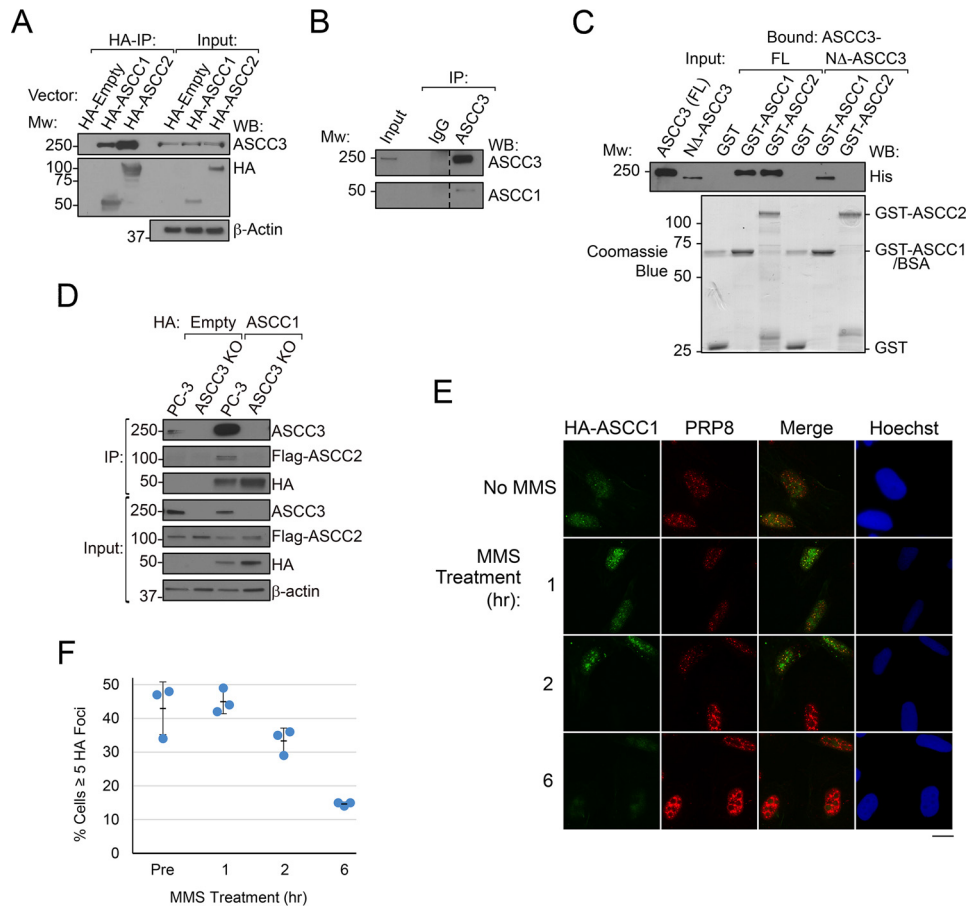
Figure 1. ASCC1 binds directly to ASCC3 but is removed from nuclear speckles upon alkylation damage. *A,* HA-tagged vector, ASCC1, or ASCC2 were expressed in 293T cells and immunoprecipitated using anti-HA resin. Immunoprecipitated (*HA-IP*) and input samples (1.5%) were analyzed using the indicated antibodies. The amount of ASCC3 immunoprecipitated by HA-ASCC1 was found to be 3.5% of the input, whereas HA-ASCC2 immunoprecipitated 8.4% of the input. Positions of molecular weight markers are shown on the *left*. *WB,* Western blot. *B,* 293T whole-cell lysate was immunoprecipitated (*IP*) using anti-ASCC3 or IgG control antibodies and then Western blotted as shown. *Input* represents 2.5% of the IP samples. *C,* GST, GST-ASCC1, or GST-ASCC2 were immobilized onto GSH-Sepharose and incubated with full-length (*FL*) His-tagged ASCC3 or an N-terminal deletion (*NΔ-ASCC3*). After washing, the bound material was analyzed by SDS-PAGE and Western blotting using anti-His antibody or by Coomassie Blue staining. *D,* HA-tagged ASCC1 was expressed in PC-3 WT or ASCC3 KO cells and immunoprecipitated using anti-HA resin. HA-IP and input samples were analyzed using the indicated antibodies. *E,* U2OS cells expressing HA-tagged ASCC1 were untreated or treated with MMS (0.5 mM) for 1, 2, or 6 h as shown. Cells were processed for immunofluorescence using anti-HA and anti-PRP8 antibodies, with Hoechst used as the nuclear counterstain. *Scale bar,* 10 μm. *F,* quantitation of *E. n* = 3 biological replicates of 100 cells for each replicate, and *error bars* indicate ± S.D. of the mean.

tion observed by microscopy, less ASCC3 was coimmunoprecipitated with ASCC2 in ASCC1 knockout cells than in WT cells upon alkylation damage (Fig. 2, *E*). Thus, ASCC1 appears to coordinate the proper recruitment of the complex components during alkylation.

Deletion analysis of ASCC1 reveals modular functional domains

We reasoned that distinct domains within ASCC1 may be responsible for the interaction with ASCC3 and its removal from the nuclear speckle domains during damage. ASCC1 contains a KH domain adjacent to an unstructured region at its N terminus, as well as an RNA ligase-like C terminus, which has been postulated to be an RNA-binding domain (22–24). We created deletion mutants of ASCC1 and tested their ability to associate with ASCC3 (Fig. 3*A*). Deletion of the N terminus of ASCC1 (ASCC1-NΔ; residues 54–357) abolished its binding to ASCC3, whereas deletion of the C terminus (ASCC1-CΔ; residues 1–243) had no effect on this interaction (Fig. 3, *A* and *B*). We then expressed the ASCC1-NΔ and ASCC1-CΔ constructs

in ASCC1 knockout cells (Fig. S2, *A* and *B*) to prevent interference from any endogenous ASCC1. We analyzed their ability to retain localization within nuclear speckles upon MMS treatment. Strikingly, HA-ASCC1-CΔ maintained foci formation, whereas HA-ASCC1-NΔ behaved like WT ASCC1 (Fig. 3, *C* and *D*). This was not because ASCC1-CΔ was expressed at a higher level than WT ASCC1 or ASCC1-NΔ (Fig. S3*A*). Thus, modular domains within ASCC1 have distinct functions during the alkylation damage response.

Putative RNA-binding domain in ASCC1 regulates ASCC function

In analyzing the C-terminal RNA ligase-like domain of ASCC1, we noticed that it contains two conserved His-Xaa-Thr motifs, shown to be important for RNA or nucleotide binding in various proteins (25). Examples of other proteins containing this motif in their nucleotide-binding pocket include the 2′–5′ RNA ligases from *Thermus thermophilus* and *Pyrococcus horikoshii,* as well as the AMP-binding protein AKAP18 (Fig. 4*A* and Fig. S3*B*) (25, 26). Previous structural studies suggest
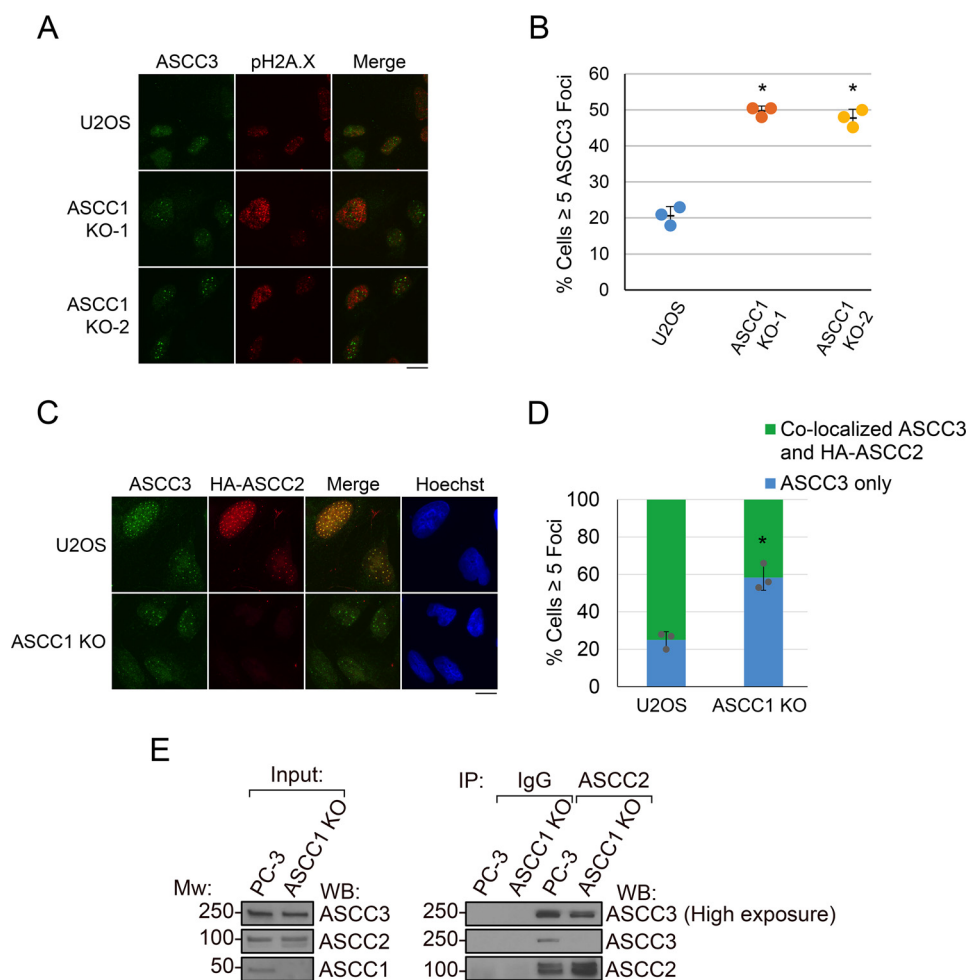
Figure 2. ASCC1 modulates alkylation-induced ASCC3 foci formation. *A,* U2OS WT and ASCC1 KO cells were treated with MMS (0.5 mM) for 6 h and processed for immunofluorescence using anti-ASCC3 and anti-pH2A.X antibodies, with Hoechst as the nuclear counterstain. *B,* quantification of *A.* $n = 3$ biological replicates of 100 cells per replicate, and *error bars* indicate ± S.D. of the mean. * = $p < 0.01$. *C,* U2OS WT and ASCC1 KO cells expressing HA-tagged ASCC2 were treated with MMS (0.5 mM) for 6 h. Cells were processed for immunofluorescence using anti-ASCC3 and anti-HA antibodies, with Hoechst as the nuclear counterstain. *Scale bars,* 10 μm. *D,* quantification of *C.* Only cells with ≥5 ASCC3 foci were scored. $n = 3$ biological replicates of 100 cells per replicate, and *error bars* indicate ± S.D. of the mean. * = $p < 0.01$. *E,* PC-3 WT and ASCC1 KO cells were treated with MMS (0.5 mM) for 6 h. Whole-cell lysate was immunoprecipitated (*IP*) using anti-ASCC2 or IgG control antibodies and then Western blotted (*WB*) as shown. *Inputs* represent 2.5% of the immunoprecipitated samples.

that these HXT motifs line the substrate-binding pocket and interact with the nucleotide through a pseudo 2-fold symmetry (27). We modeled this domain within ASCC1 using the Phyre2 server (28, 29). The resulting structural analysis suggested that it forms a similar overall structure to other members of the 2H phosphoesterase family (Fig. 4B) (30). Furthermore, the predicted structure suggests that the conserved HXT motifs of ASCC1 are positioned such that they also line a putative nucleotide- or RNA-binding pocket similar to the aforementioned RNA ligases and AKAP18. Notably, the ASCC1 domain lacks residues critical for ligase activity (Fig. S3C) (31). We then mutated both of the HXT motifs of ASCC1 to AXA (ASCC1-AXA: ^{179}HLT → ^{179}ALA and ^{277}HAT → ^{277}AAA) and analyzed its localization during MMS damage. As with ASCC1-CΔ, ASCC1-AXA retained foci under these conditions (Fig. 4, *C* and *D*, Fig. S3, *D–F*). This indicates that the HXT motifs of ASCC1 play a role in its localization during alkylation damage.

Because the C terminus of ASCC1 appeared to be critical for regulating its ability to form foci, we asked whether the RNA ligase-like domain played a role in foci formation of other com-

plex components during alkylation damage. To address this question, we rescued ASCC1 knockout cells by expressing exogenous ASCC1 WT, ASCC1-CΔ, or ASCC1-AXA (Fig. S3G). Although the WT ASCC1 partially rescued HA-ASCC2/ ASCC3 foci colocalization, neither ASCC1-CΔ nor ASCC1-AXA was able to rescue this phenotype (Fig. 4, *E* and *F*). Thus, this putative RNA ligase-like domain of ASCC1 plays an important role in the regulation of the ASCC complex localization upon alkylation damage.

Role of ASCC1 in alkylation damage resistance

The previous results suggested that ASCC1 may play a key role in modulating ASCC recruitment during alkylation damage. We then tested whether ASCC1 was functionally important for alkylation damage resistance in PC-3 prostate cancer cells. ASCC1 was knocked out in these cells using CRISPR/Cas9 (Fig. S2E). Loss of ASCC1 resulted in an increase in sensitivity to MMS in these cells (Fig. 5A). Again, the increase in sensitivity was observed with two distinct ASCC1 knockout clones. To determine whether this decrease in cell survival in response to
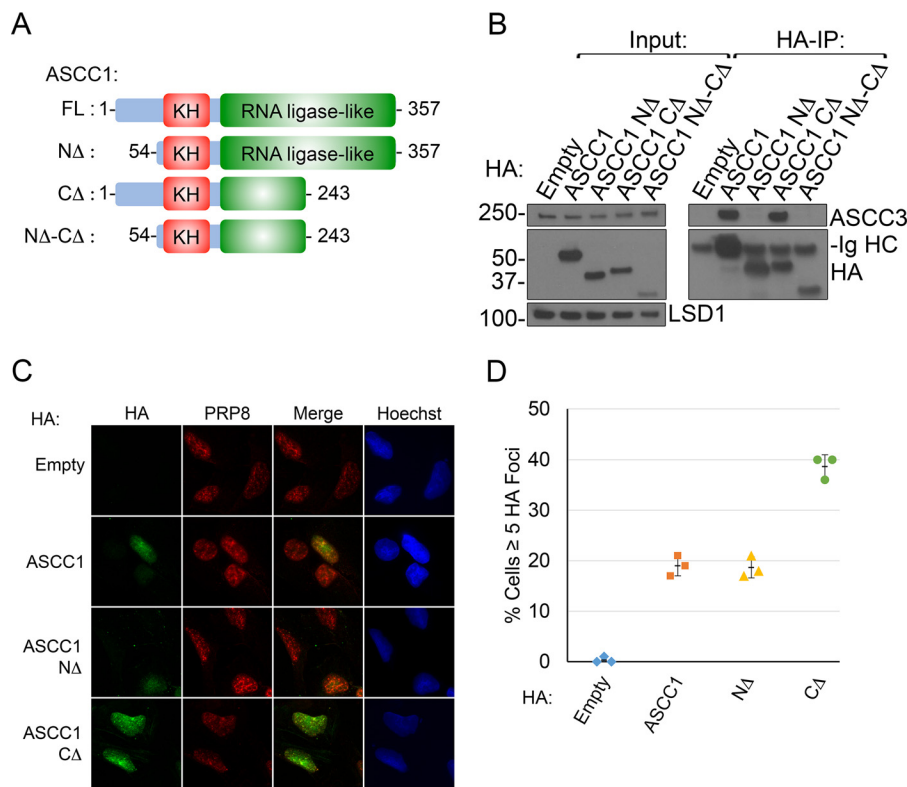
Figure 3. Deletion analysis of ASCC1 reveals modular functional domains. *A,* schematic of human ASCC1 domain structure and mutants (to scale). *B,* HA-tagged ASCC1 FL or indicated ASCC1 deletions were expressed in 293T cells and immunoprecipitated using anti-HA resin. Immunoprecipitated (*IP*) HA-IP and input samples were analyzed using the indicated antibodies. *C,* U2OS ASCC1 KO cells expressing HA-tagged ASCC1 or indicated ASCC deletions were treated with MMS (0.5 mM) for 6 h. Cells were processed for immunofluorescence using anti-HA and anti-PRP8 antibodies, with Hoechst used as the nuclear counter stain. *Scale bars*, 10 μm. *D,* quantification of *C. n* = 3 biological replicates of 100 cells per replicate, and *error bars* indicate ± S.D. of the mean.

MMS was due to the function of ASCC1 within the ASCC complex, or whether this was due to its function in another pathway, we created ASCC1–ASCC3 double knockout cells (ASCC1/3 DKO). We sequentially knocked out ASCC3 in PC-3 cells and then knocked out ASCC1 using CRISPR/Cas9 (Figs. S1*B* and S4, *A* and *B*). MMS sensitivity of all four resulting genotypes was then tested. Consistent with our previous work, loss of ASCC3 increased sensitivity to MMS (18). However, the ASCC1/3 DKO cells did not have an increase in MMS sensitivity compared with either the ASCC1 KO or the ASCC3 KO cells (Fig. 5*B*). These results support the notion that ASCC1 has an epistatic relationship with ASCC3 in alkylation damage resistance. Taken together, our data support a role for ASCC1 in controlling the ASCC complex recruitment and function during the cellular response to alkylation damage.

Discussion

We recently described a signaling pathway that is activated by alkylation damage to recruit the ALKBH3–ASCC complex to nuclear foci (21). This pathway depends upon the RNF113A E3 ligase, which induces Lys-63–linked ubiquitination that is then recognized by the ASCC2 subunit (21). Here, we present evidence for additional regulation of this pathway by ASCC1. Our work suggests that ASCC1 is constitutively present at nuclear speckle foci prior to damage, but leaves these foci upon MMS treatment. In addition, ASCC1 can interact directly with ASCC3 and thus can modulate its localization during alkylation damage. Consistent with a role in this pathway, knockout of

ASCC1 sensitizes cells to alkylation damage. Loss of ASCC1 does not further increase the sensitivity of cells that lack ASCC3, suggesting that the role of ASCC1 in the alkylation damage response is primarily through the ASCC complex.

Surprisingly, unlike ASCC2 or ASCC3, ASCC1 is already present at nuclear foci in the absence of any damage. Upon alkylation damage, ASCC1 is removed from these foci (Fig. 1, *E* and *F*). This phenomenon depends on the C-terminal domain of ASCC1 and, more specifically, its H*X*T motifs (Figs. 3 and 4). At the same time, ASCC1 can bind directly to ASCC3 via its N terminus (Fig. 1, *A*–*C*). This physical interaction and the dynamic localization of ASCC1 during alkylation set up our preferred model to explain the resulting phenotypes from ASCC1-deficient cells (Fig. 5*C*). We hypothesize that ASCC1 is acting as a specificity determinant for ASCC3 localization at these foci. In WT cells, we observe that the vast majority of the ASCC3 foci are positive for ASCC2 (Fig. 2, *C* and *D*). In the ASCC1 knockout cells, ASCC3 foci are significantly increased, yet the majority of these lack ASCC2. Thus, there are likely two subsets of ASCC3 foci: those that are positive for ASCC2 and those that are negative for ASCC2. In WT cells, the fraction of ASCC3 present at foci without ASCC2 is likely removed in a manner dependent on ASCC1. This is consistent with why we observe more ASCC3 foci in ASCC1 knockout cells. The failure of ASCC3 to be removed from these ASCC2-negative foci by ASCC1 would explain why we observe more ASCC3 foci that lack ASCC2 in the ASCC1 knockout cells. Our
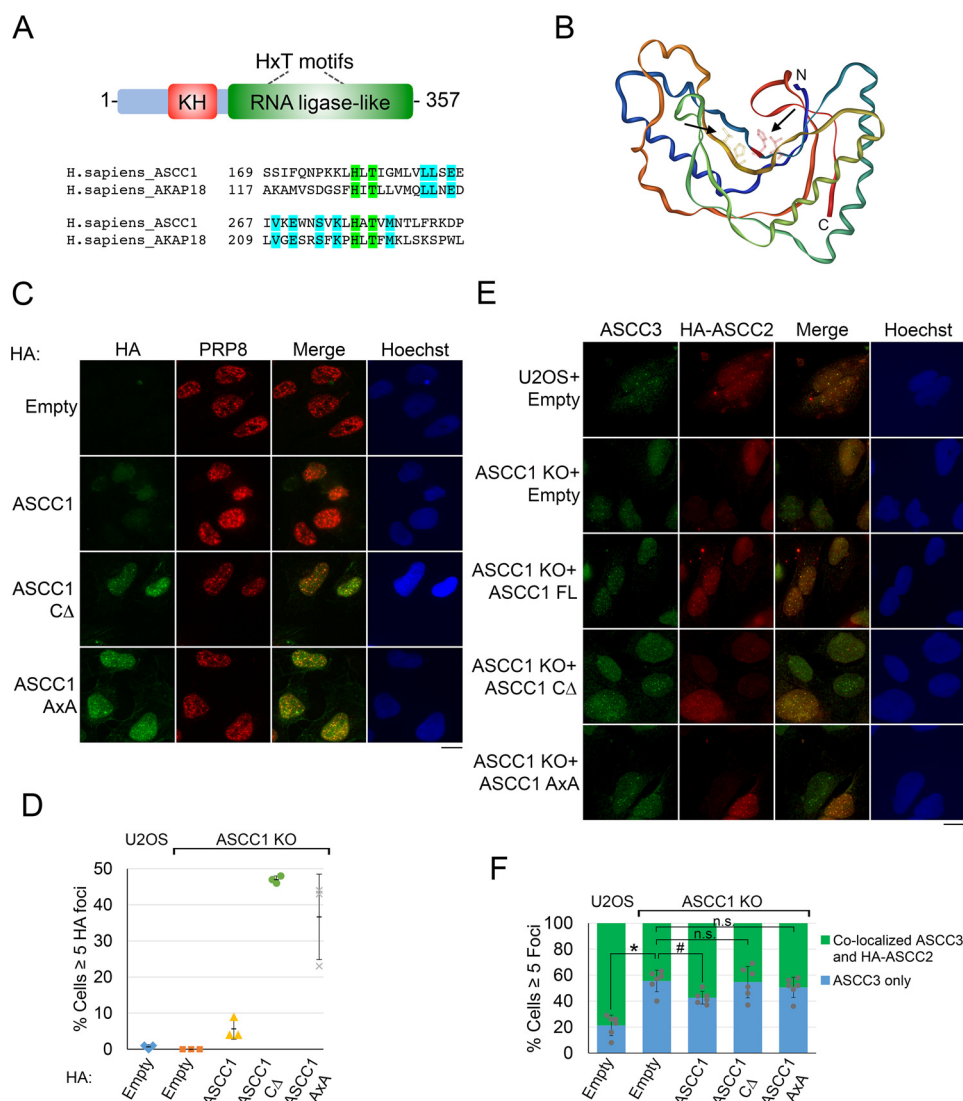
Figure 4. Putative RNA-binding domain in ASCC1 regulates ASCC function. *A,* schematic of the human ASCC1 protein is shown on *top*, with the positions of the HXT motifs (to scale). Sequence alignment with human AKAP18 is shown on *bottom*. The dual HXT motifs are highlighted in *green*, and neighboring conserved residues are highlighted in *blue. B,* predicted structure of ASCC1 (residues 132–355). The HXT motifs are indicated by *arrows.* This domain was modeled using the Phyre2 server. *C,* U2OS WT and ASCC1 KO cells expressing HA-tagged ASCC1 or indicated ASCC deletions were treated with MMS (0.5 mM) for 6 h. Cells were processed for immunofluorescence using anti-HA and anti-PRP8 antibodies, with Hoechst used as the nuclear counterstain. *D,* quantification of *C.* Only cells with ≥5 ASCC3 foci were scored. $n = 3$ biological replicates of 100 cells, and *error bars* indicate ± S.D. of the mean. *E,* U2OS WT and ASCC1 KO cells expressing HA-tagged ASCC2 and untagged ASCC1 WT or indicated mutations were treated with MMS (0.5 mM) for 6 h. Cells were processed for immunofluorescence using anti-HA and anti-ASCC3 antibodies, with Hoechst used as the nuclear counterstain. *Scale bars,* 10 μm. *F,* quantification of *E.* $n = 6$ biological replicates of 100 cells, and *error bars* indicate ± S.D. of the mean. * = $p < 0.001$; # = $p < 0.05$; *n.s.,* not significant.

immunoprecipitation results further confirm this notion (Fig. 2E).

Why does an increase in ASCC3 foci formation lead to increased alkylation damage sensitivity? This phenotype is potentially due to the necessary regulation of ASCC3 recruitment by ASCC1. In double-stranded break repair, the loss of the repair protein 53BP1 increases BRCA1 recruitment, but this leads to increased sensitivity to γ-irradiation, at least partly due to the recruitment of BRCA1 in the G_1 phase of the cell cycle (32). This inappropriate recruitment and attempt at homologous recombination in G_1 is thought to be deleterious in double-strand break repair. In a like manner, in the absence of ASCC1, inappropriate ASCC3 recruitment may cause alkylation damage sensitivity because other repair factors are displaced, or a portion of ASCC3 needs to be removed for repair to

be promptly completed. It is also possible that in the absence of ASCC1, the complex cannot function properly, and alkylation damage sensitivity is increased despite an increase in ASCC3 recruitment.

The C-terminal RNA ligase-like domain of ASCC1, which appears to be critical for the function described here, is part of a larger 2H phosphoesterase family of enzymes that have been shown to harbor diverse activities, including *bona fide* tRNA ligases, phosphodiesterases, and putative RNA-binding factors (26, 30). Structural studies on the phosphoesterase domain of AKAP18 initially suggested a proclivity for binding to AMP and CMP in a manner that depends upon its HXT motifs (27). It is intriguing that AKAP18 binds to the same nucleotides that are the major reaction products for the ALKBH3 dealkylase activity, which primarily targets 1-methyladenine and 3-methylcy-
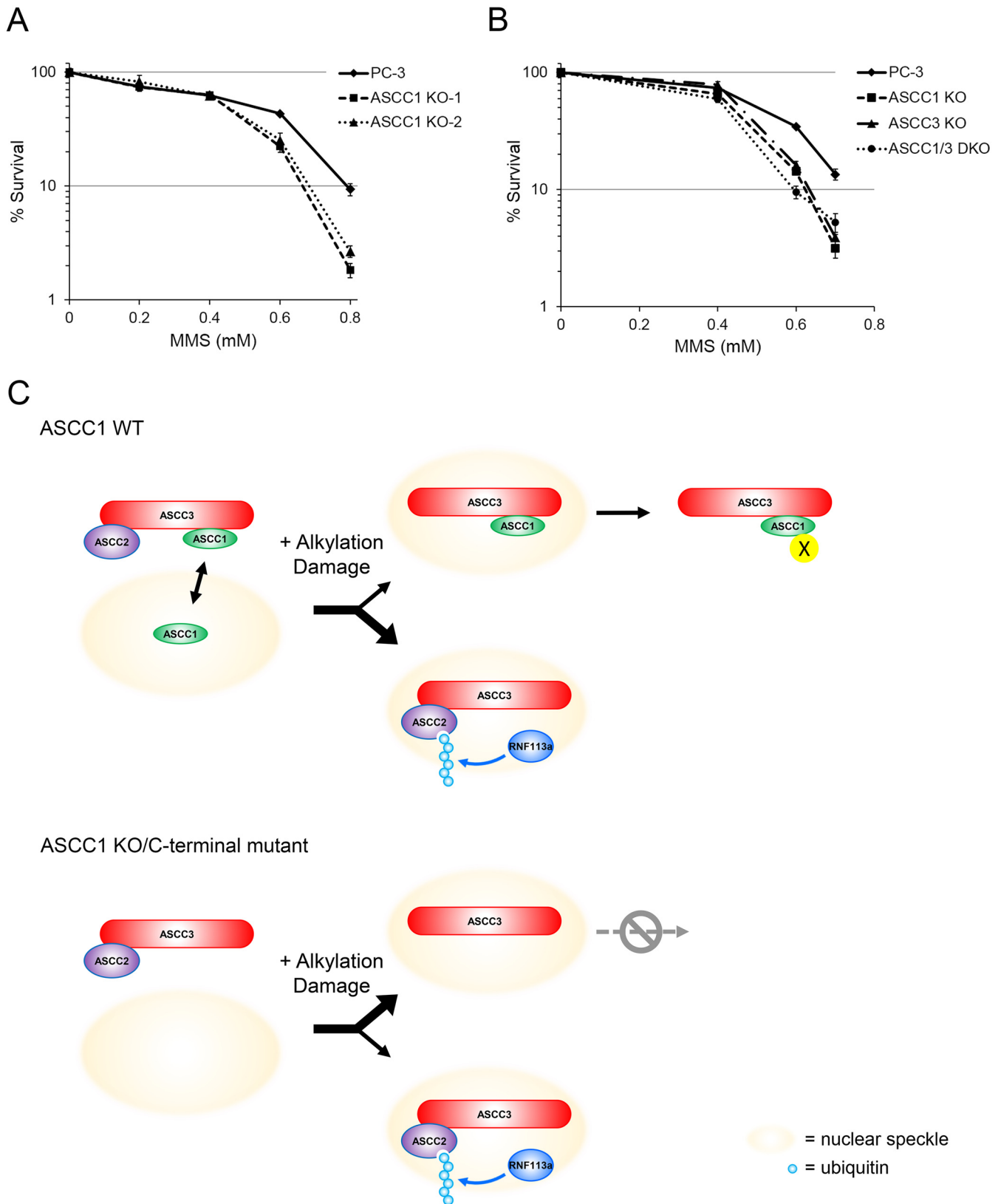
Figure 5. ASCC1 KO cells are sensitive to alkylation damage. *A,* PC-3 ASCC1 KO cells were assessed for sensitivity to MMS relative to WT PC-3 cells. Cell survival was measured by MTS assay. *n* = 5, and *error bars* indicate ± S.D. of the mean. *B,* PC-3 ASCC1 KO, ASCC3 KO, and ASCC1/3 DKO cells were assessed for sensitivity to MMS relative to WT PC-3 cells. Cell survival was measured by MTS assay. *n* = 5, and *error bars* indicate ± S.D. of the mean. *C,* proposed model for ASCC complex localization during alkylation damage. In WT cells (36), RNF113a-mediated ubiquitination is recognized by ASCC2 and recruits ASCC3 to nuclear speckle foci. Simultaneously, a fraction of ASCC3 is recruited to ASCC2-negative foci, but these are removed by ASCC1. This activity of ASCC1 depends upon the C-terminal RNA ligase-like domain via the engagement of an unknown ligand (*X*). In ASCC1 KO/C-terminal mutant cells (*bottom*), the fraction of ASCC3 foci that are independent of ASCC2 is significantly increased. See text for details.

tosine for demethylation. We currently do not have any direct evidence for the binding of ASCC1 to AMP or CMP. However, the importance of this domain in ASCC1 foci formation strongly implies that substrate binding through this domain, whatever its biochemical identity, plays a role in ASCC complex recruitment and function.

Experimental procedures

Plasmids

Human ASCC1 cDNA was isolated by RT-PCR from total human RNA, cloned into pENTR-3C (Invitrogen), and subcloned into pMSCV-FLAG, pMSCV-FLAG-HA, or pHAGE-CMV-HA$_3$ by Gateway recombination (33). ASCC1 deletions and point mutations were created by PCR and cloned as above. ASCC2, ASCC3, and ALKBH3 vectors were previously described (21). For recombinant protein expression, WT ASCC1, ASCC1 mutants, and ASCC2 were subcloned into pGEX-4T1 or pET28a-FLAG. For expressing the His$_6$-tagged full-length ASCC3 and NΔ-ASCC3 (401–2202), the pENTR-3C vectors containing these cDNAs were subcloned into pDEST10 (Invitrogen). All constructs produced by PCR were verified by Sanger sequencing.

CRISPR/Cas9-mediated knockouts

U2OS and PC-3 KO cells were created using CRISPR/Cas9 genome editing at the Genome Engineering and iPSC Center (GEiC) at Washington University School of Medicine (St. Louis). The U2OS ASCC3 KO cells were previously described (21). The gRNA sequences used to generate the ASCC1 KO cell lines were 5′-AAGGATTCCGGTCTACTTTGNGG-3′ and 5′-AAGTAGACCGGAATCCTTGTNGG-3′. The gRNA sequence used to generate the PC-3 ASCC3 KO cell line was 5′-GACATTTGAAAAGGAACGCANGG-3′. All knockout clones were verified by deep sequencing or by Western blot analysis.

Cell culture, viral transduction, and cell survival assays

U2OS, PC-3, 293T, and Sf9 cells were cultured and maintained as described previously (34). Preparation of viruses, transfection, and viral transduction were also performed as described previously (34). For knockout cell foci rescue experiments, U2OS cells were transduced with WT ASCC1 or ASCC1 mutants using the pMSCV retroviral vector and pHAGE-CMV-HA$_3$-ASCC2. For DNA damaging agent survival assays using PC-3 cells, 4000–15,000 cells/well were cultured overnight in 96-well plates in 100 μl of media. Cells were then exposed to medium containing the indicated concentration of MMS (Sigma) for 24 h at 37 °C. The media were then replaced with normal media, and cell viability was assessed 72 h after initial exposure to MMS via the MTS assay (Promega). All MTS-based survival experiments were carried out in quintuplicate.

Recombinant protein purification

For purification of the His$_6$-tagged ASCC3 and NΔ-ASCC3, the baculovirus vector was produced using the Bac-to-Bac expression system (ThermoFisher Scientific). Amplified baculovirus was used to infect Sf9 cells and harvested after 72 h. The cells were resuspended in Buffer L (20 mM Tris, pH 7.3, 150 mM NaCl, 8% glycerol, 0.2% Nonidet P-40, 0.1% Triton X-100, 20 mM imidazole) plus protease inhibitors and frozen −80 °C. Cells were lysed by sonication and rotated for 30 min at 4 °C. The cell extracts were then centrifuged at 10,000 rpm for 10 min. The supernatant was incubated with nickel-nitrilotri-acetic acid beads and eluted with Buffer L containing 400 mM imidazole. His-ASCC1 and GST-tagged recombinant proteins were purified from *E. coli* as described (34). All proteins were dialyzed into TAP buffer (50 mM Tris, pH 7.9, 100 mM KCl, 5 mM MgCl$_2$, 0.2 mM EDTA, 0.1% Nonidet P-40, 10% glycerol, 2 mM 2-mercaptoethanol, 0.2 mM phenylmethylsulfonyl fluoride) after purification.

Protein binding assays

All *in vitro* GST–protein binding assays were performed as described previously (35) with minor modifications. Briefly, 5 μg of GST-tagged bait protein was incubated with 10 μl of GSH-Sepharose beads and 250 ng of His$_6$ ASCC3 FL or NΔ-ASCC3, 1 μg of His$_6$ ASCC1, or 500 ng of Lys-63–Ub(3–7) in TAP buffer containing 1% BSA in a total volume of 100 μl. After incubation at 4 °C with rotation for 1 h, beads were washed extensively using TAP buffer. Bound material was eluted using Laemmli buffer and analyzed by SDS-PAGE and Western blotting.

Structural model

The model for the predicted structure of ASCC1 was generated using the publicly available Phyre2 server (28, 29).

Statistical analysis

All *p* values were calculated by the unpaired two-tailed Student's *t* test.

Immunofluorescence microscopy

All immunofluorescence microscopy was done as described previously (21, 35). 100 cells were analyzed at least in biological triplicate for all quantifications.

Immunoprecipitation and Western blotting

Immunoprecipitation of HA-tagged ASCC1, ASCC1 mutants, and ASCC2 was performed by transfection of constructs into 293T cells using Transit293 reagent (Mirus Bio). Cells were treated with 0.5 mM MMS as indicated, collected, washed in 1× PBS, and frozen at −80 °C. Cell pellets were resuspended in IP lysis buffer (50 mM Tris, pH 7.9, 300 mM NaCl, 10% glycerol, 1% Triton X-100, 1 mM DTT, and protease inhibitors), lysed by sonication, and cleared by centrifugation. An equal volume of IP lysis buffer containing no salt was added (final concentration of NaCl was 150 mM). Lysates were then incubated with anti-HA resin (Santa Cruz Biotechnology) for 3–4 h at 4 °C with rotation. The beads were washed extensively with IP lysis buffer containing 150 mM NaCl, and bound material was eluted with Laemmli buffer.

Preparation of viruses, transfection, and viral transduction for immunoprecipitation of HA-tagged ASCC1 or HA-empty from PC-3 WT and ASCC3 KO cells was performed as

described previously (34). Cells were selected with 1 μg/ml puromycin for 24 h. The media were then replaced with normal media for 2 days, after which cells were transfected with FLAG-ASCC2. Cells were collected and washed in 1× PBS and frozen at −80 °C 2 days after transfection. Immunoprecipitation was then executed as described above.

Endogenous immunoprecipitation was carried out by collecting the cells and freezing at −80 °C as above. Cell pellets were resuspended in TAP buffer containing 300 mM KCl, lysed by sonication, and cleared by centrifugation. IP lysis buffer containing no salt was added to bring the final concentration of KCl to 100 mM. Samples were pre-cleared by incubation with protein A/G beads (Santa Cruz Biotechnology) with rotation at 4 °C. After centrifugation, the supernatant was then incubated with the relevant antibodies overnight at 4 °C. Protein A/G beads were then added and rotated at 4 °C for 1 h. The samples were then centrifuged and washed extensively with TAP buffer. Bound material was eluted with Laemmli buffer and analyzed by Western blotting. All antibodies and concentrations used in this study are shown in Table S1.

References

1. Sedgwick, B., Bates, P. A., Paik, J., Jacobs, S. C., and Lindahl, T. (2007) Repair of alkylated DNA: recent advances. *DNA Repair* **6,** 429–442 CrossRef Medline
2. Fu, D., Calvo, J. A., and Samson, L. D. (2012) Balancing repair and tolerance of DNA damage caused by alkylating agents. *Nat. Rev. Cancer* **12,** 104–120 CrossRef Medline
3. Drabløs, F., Feyzi, E., Aas, P. A., Vaagbø, C. B., Kavli, B., Bratlie, M. S., Peña-Diaz, J., Otterlei, M., Slupphaug, G., and Krokan, H. E. (2004) Alkylation damage in DNA and RNA—repair mechanisms and medical significance. *DNA Repair* **3,** 1389–1407 CrossRef Medline
4. Soll, J. M., Sobol, R. W., and Mosammaparast, N. (2017) Regulation of DNA alkylation damage repair: lessons and therapeutic opportunities. *Trends Biochem. Sci.* **42,** 206–218 CrossRef Medline
5. Krokan, H. E., and Bjorås, M. (2013) Base excision repair. *Cold Spring Harb. Perspect. Biol.* **5,** a012583 CrossRef Medline
6. Xu-Welliver, M., and Pegg, A. E. (2002) Degradation of the alkylated form of the DNA repair protein, O(6)-alkylguanine-DNA alkyltransferase. *Carcinogenesis* **23,** 823–830 CrossRef Medline
7. Zak, P., Kleibl, K., and Laval, F. (1994) Repair of O6-methylguanine and O4-methylthymine by the human and rat O6-methylguanine-DNA methyltransferases. *J. Biol. Chem.* **269,** 730–733 Medline
8. Falnes, P. Ø., Johansen, R. F., and Seeberg, E. (2002) AlkB-mediated oxidative demethylation reverses DNA damage in *Escherichia coli. Nature* **419,** 178–182 CrossRef Medline
9. Trewick, S. C., Henshaw, T. F., Hausinger, R. P., Lindahl, T., and Sedgwick, B. (2002) Oxidative demethylation by *Escherichia coli* AlkB directly reverts DNA base damage. *Nature* **419,** 174–178 CrossRef Medline
10. Gerken, T., Girard, C. A., Tung, Y. C., Webby, C. J., Saudek, V., Hewitson, K. S., Yeo, G. S., McDonough, M. A., Cunliffe, S., McNeill, L. A., Galvanovskis, J., Rorsman, P., Robins, P., Prieur, X., Coll, A. P., *et al.* (2007) The obesity-associated FTO gene encodes a 2-oxoglutarate-dependent nucleic acid demethylase. *Science* **318,** 1469–1472 CrossRef Medline
11. Kurowski, M. A., Bhagwat, A. S., Papaj, G., and Bujnicki, J. M. (2003) Phylogenomic identification of five new human homologs of the DNA repair enzyme AlkB. *BMC Genomics* **4,** 48 CrossRef Medline
12. Sanchez-Pulido, L., and Andrade-Navarro, M. A. (2007) The FTO (fat mass and obesity associated) gene codes for a novel member of the non-heme dioxygenase superfamily. *BMC Biochem.* **8,** 23 CrossRef Medline
13. Duncan, T., Trewick, S. C., Koivisto, P., Bates, P. A., Lindahl, T., and Sedgwick, B. (2002) Reversal of DNA alkylation damage by two human dioxygenases. *Proc. Natl. Acad. Sci. U.S.A.* **99,** 16660–16665 CrossRef Medline
14. Gros, L., Maksimenko, A. V., Privezentzev, C. V., Laval, J., and Saparbaev, M. K. (2004) Hijacking of the human alkyl-*N*-purine-DNA glycosylase by 3,*N*4-ethenocytosine, a lipid peroxidation-induced DNA adduct. *J. Biol. Chem.* **279,** 17723–17730 CrossRef Medline
15. Lingaraju, G. M., Davis, C. A., Setser, J. W., Samson, L. D., and Drennan, C. L. (2011) Structural basis for the inhibition of human alkyladenine DNA glycosylase (AAG) by 3,*N*4-ethenocytosine-containing DNA. *J. Biol. Chem.* **286,** 13205–13213 CrossRef Medline
16. Fu, D., and Samson, L. D. (2012) Direct repair of 3,*N*(4)-ethenocytosine by the human ALKBH2 dioxygenase is blocked by the AAG/MPG glycosylase. *DNA Repair* **11,** 46–52 CrossRef Medline
17. Jung, D. J., Sung, H. S., Goo, Y. W., Lee, H. M., Park, O. K., Jung, S. Y., Lim, J., Kim, H. J., Lee, S. K., Kim, T. S., Lee, J. W., and Lee, Y. C. (2002) Novel transcription coactivator complex containing activating signal cointegrator 1. *Mol. Cell. Biol.* **22,** 5203–5211 CrossRef Medline
18. Dango, S., Mosammaparast, N., Sowa, M. E., Xiong, L. J., Wu, F., Park, K., Rubin, M., Gygi, S., Harper, J. W., and Shi, Y. (2011) DNA unwinding by ASCC3 helicase is coupled to ALKBH3-dependent DNA alkylation repair and cancer cell proliferation. *Mol. Cell* **44,** 373–384 CrossRef Medline
19. Konishi, N., Nakamura, M., Ishida, E., Shimada, K., Mitsui, E., Yoshikawa, R., Yamamoto, H., and Tsujikawa, K. (2005) High expression of a new marker PCA-1 in human prostate carcinoma. *Clin. Cancer Res.* **11,** 5090–5097 CrossRef Medline
20. Tasaki, M., Shimada, K., Kimura, H., Tsujikawa, K., and Konishi, N. (2011) ALKBH3, a human AlkB homologue, contributes to cell survival in human non-small-cell lung cancer. *Br. J. Cancer* **104,** 700–706 CrossRef Medline
21. Brickner, J. R., Soll, J. M., Lombardi, P. M., Vågbø, C. B., Mudge, M. C., Oyeniran, C., Rabe, R., Jackson, J., Sullender, M. E., Blazosky, E., Byrum, A. K., Zhao, Y., Corbett, M. A., Gécz, J., Field, M., *et al.* (2017) A ubiquitin-dependent signalling axis specific for ALKBH-mediated DNA dealkylation repair. *Nature* **551,** 389–393 CrossRef Medline
22. Brown, R. L., August, S. L., Williams, C. J., and Moss, S. B. (2003) AKAP7γ is a nuclear RI-binding AKAP. *Biochem. Biophys. Res. Commun.* **306,** 394–401 CrossRef Medline
23. Siomi, H., Matunis, M. J., Michael, W. M., and Dreyfuss, G. (1993) The pre-mRNA binding K protein contains a novel evolutionarily conserved motif. *Nucleic Acids Res.* **21,** 1193–1198 CrossRef Medline
24. Valverde, R., Edwards, L., and Regan, L. (2008) Structure and function of KH domains. *FEBS J.* **275,** 2712–2726 CrossRef Medline
25. Koonin, E. V., and Gorbalenya, A. E. (1990) Related domains in yeast tRNA ligase, bacteriophage T4 polynucleotide kinase and RNA ligase, and mammalian myelin 2′,3′-cyclic nucleotide phosphohydrolase revealed by amino acid sequence comparison. *FEBS Lett.* **268,** 231–234 CrossRef Medline
26. Mazumder, R., Iyer, L. M., Vasudevan, S., and Aravind, L. (2002) Detection of novel members, structure-function analysis and evolutionary classifica-

tion of the 2H phosphoesterase superfamily. *Nucleic Acids Res.* **30,** 5229–5243 CrossRef Medline

27. Gold, M. G., Smith, F. D., Scott, J. D., and Barford, D. (2008) AKAP18 contains a phosphoesterase domain that binds AMP. *J. Mol. Biol.* **375,** 1329–1343 CrossRef Medline

28. Kelley, L. A., and Sternberg, M. J. (2009) Protein structure prediction on the Web: a case study using the Phyre server. *Nat. Protoc.* **4,** 363–371 CrossRef Medline

29. Kelley, L. A., Mezulis, S., Yates, C. M., Wass, M. N., and Sternberg, M. J. (2015) The Phyre2 web portal for protein modeling, prediction and analysis. *Nat. Protoc.* **10,** 845–858 CrossRef Medline

30. Silverman, R. H., and Weiss, S. R. (2014) Viral phosphodiesterases that antagonize double-stranded RNA signaling to RNase L by degrading 2–5A. *J. Interferon Cytokine Res.* **34,** 455–463 CrossRef Medline

31. Doherty, A. J., and Suh, S. W. (2000) Structural and mechanistic conservation in DNA ligases. *Nucleic Acids Res.* **28,** 4051–4058 CrossRef Medline

32. Daley, J. M., and Sung, P. (2014) 53BP1, BRCA1, and the choice between recombination and end joining at DNA double-strand breaks. *Mol. Cell. Biol.* **34,** 1380–1388 CrossRef Medline

33. Sowa, M. E., Bennett, E. J., Gygi, S. P., and Harper, J. W. (2009) Defining the human deubiquitinating enzyme interaction landscape. *Cell* **138,** 389–403 CrossRef Medline

34. Zhao, Y., Majid, M. C., Soll, J. M., Brickner, J. R., Dango, S., and Mosammaparast, N. (2015) Noncanonical regulation of alkylation damage resistance by the OTUD4 deubiquitinase. *EMBO J.* **34,** 1687–1703 CrossRef Medline

35. Mosammaparast, N., Kim, H., Laurent, B., Zhao, Y., Lim, H. J., Majid, M. C., Dango, S., Luo, Y., Hempel, K., Sowa, M. E., Gygi, S. P., Steen, H., Harper, J. W., Yankner, B., and Shi, Y. (2013) The histone demethylase LSD1/KDM1A promotes the DNA damage response. *J. Cell Biol.* **203,** 457–470 CrossRef Medline

36. Eadie, J. S., Conrad, M., Toorchen, D., and Topal, M. D. (1984) Mechanism of mutagenesis by O6-methylguanine. *Nature* **308,** 201–203 CrossRef Medline

SASBMB

RNA ligase-like domain in activating signal cointegrator 1 complex subunit 1 (ASCC1) regulates ASCC complex function during alkylation damage

Jennifer M. Soll, Joshua R. Brickner, Miranda C. Mudge and Nima Mosammaparast